PHYSICAL REVIEW D **87,** 095002 (2013)

QCD parity violation at LHC in warped extra dimension

Naoyuki Haba,[1] Kunio Kaneta,[1,2] and Soshi Tsuno[3]

[1]*Department of Physics, Faculty of Science, Hokkaido University, Sapporo 060-0810, Japan*
[2]*Department of Physics, Osaka University, Toyonaka, Osaka 560-0043, Japan*
[3]*High Energy Accelerator Research Organization (KEK), Tsukuba, Ibaraki 305-0801, Japan*

(Received 5 December 2012; published 6 May 2013)

An extra dimension is one of the most attractive candidates beyond the Standard Model. In warped extra dimensional space-time, not only the gauge hierarchy problem but also quark-lepton mass hierarchy can be naturally explained. In this setup, a sizable parity violation through a Kaluza-Klein gluon exchange appears in the QCD process such as helicity dependent top pair production. We investigate this QCD parity violating process by use of the $SO(5) \times U(1)$ gauge-Higgs unification model. We evaluate LHC observable quantities, i.e., a charge asymmetry and a forward-backward asymmetry of the top pair production, and find that a sizable charge asymmetry can be observed with specific model parameters.

DOI: 10.1103/PhysRevD.87.095002 PACS numbers: 14.80.Rt, 13.88.+e, 14.65.Ha

I. INTRODUCTION

ATLAS and CMS collaborations at the LHC reported a discovery of a new boson which is consistent with the Standard Model (SM) Higgs boson [1]. It is important that the observed boson can be really identified to the SM Higgs boson. On the other hand, a stabilization of Higgs self coupling requires an underlying theory behind the SM [2,3] (see also Ref. [4] and references therein). Supersymmetry (SUSY) and an extra dimension are the most promising candidates beyond the SM, which naturally contain stable dark matter particles. For a warped extra dimension, which is first proposed by Randall and Sundrum (RS) in Ref. [5], provides a framework which solves the hierarchy problem. In the original model, the SM fields are localized to a brane. However, when the SM fermions and gauge bosons propagate in the bulk, models have attractive features such as explaining fermion mass hierarchy (see, for example Ref. [6]). In this setup, configuration of the SM fermion wave function depends on bulk mass parameters c_i, where i is a label of fermion. Fermions with $c_i > 1/2$ are localized near the Planck brane, while the ones with $c_i < 1/2$ are localized near the TeV brane. Since the Higgs is localized to the TeV brane, a mass of fermions with $c_i > 1/2$ is smaller than that of fermions with $c_i < 1/2$ due to an overlap of wave functions among the Higgs and fermions. In general, c_i of left-handed fermions are not the same as those of right-handed fermions [7]. Focusing attention on the QCD sector, the nth Kaluza-Klein (KK) gluon $G^{(n)}$ is localized to the TeV brane. Therefore, overlap between $G^{(n)}$ and q_L is different from that between $G^{(n)}$ and q_R [8]. This means that parity violation in the QCD process is accommodated in a warped extra dimension scenario.

Parity violation in the QCD process can be measured by using helicity dependent top pair production. Helicity measurement of $t\bar{t}$ is shown in Ref. [9]. In the SM QCD sector, of course, there is no parity violation in top pair production. The SM background is induced by electroweak interaction [10,11]. The $t\bar{t}$ helicity asymmetry is expected to be highly sensitive to new physics. For example, SUSY can also arise sizable $t\bar{t}$ asymmetry through squark loop diagrams, because $\tilde{q}_L$ and $\tilde{q}_R$ have different a mass spectrum in general, and $q_{L(R)}$-$\tilde{q}_{L(R)}$-$\tilde{g}$ is a chiral interaction [11]. For another QCD parity violating process, quarkonium decay is investigated in Ref. [12]. Comparing to the SUSY models, the warped extra dimension model has much larger QCD parity violation due to an existence of tree level contributions.

In this paper, we investigate the QCD parity violation by use of $SO(5) \times U(1)$ gauge-Higgs unification model as an example of warped extra dimension scenario with bulk quark configurations. Gauge-Higgs unification is an attractive scenario which can explain the origin of the Higgs boson with finite mass, and the $SO(5) \times U(1)$ model is a realistic setup [13]. In this model, Higgs and $G^{(n)}$ are localized to the TeV-brane, and $q_L(q_R)$ is typically located near the Planck (the TeV) brane [14].[1] We investigate helicity asymmetry of top pair production. It was also researched in Ref. [8], however, we will evaluate it by use of LHC observables, i.e., a charge asymmetry and a forward-backward asymmetry here. We will find that a sizable charge asymmetry can be observed with specific model parameters.

This paper is organized as follows. In Sec. II, we give a brief review of $SO(5) \times U(1)$ gauge-Higgs unification model. In Sec. III, we analyze the $t\bar{t}$ left-right asymmetry $A_{\rm LR}$, which can be observed by a charge asymmetry A_C, and a forward-backward asymmetry $A_{\rm FB}$ in the LHC experiment. We present a conclusion in Sec. IV.

[1]In general, configuration of quark wave functions are also different among their flavor. Thus, a different configuration between q_L and q_R induces not only parity violation but also flavor violation. Constraints from flavor violation are studied in Ref. [15].

 © 2013 American Physical Society

II. $SO(5) \times U(1)$ GAUGE-HIGGS UNIFICATION MODEL

We pick up the $SO(5) \times U(1)$ gauge-Higgs unification model as a warped extra dimension scenario in which Higgs and KK gluon are localized to the TeV brane and left- and right-handed fermions have different configurations in the bulk. The model is constructed in the RS warped space-time [5], which metric is given by

$$ds^2 = e^{-2\sigma(y)}\eta_{\mu\nu}dx^\mu dx^\nu + dy^2, \tag{2.1}$$

where $\sigma(y) = k|y|$ with 5-dimensional (5D) scalar curvature k. The fifth dimension y is orbifolded on S^1/Z_2, and the region of y is given by $0 \le y \le L$. The Planck and the TeV brane are located at $y = 0$ and $y = L$, respectively. The gauge group of this model is $SO(5) \times U(1)_X \times SU(3)_C$ in the bulk, and $SO(5) \times U(1)_X$ is reduced to $SU(2)_L \times SU(2)_R \times U(1)_X$ by orbifold boundary conditions. The $SU(2)_R \times U(1)_X$ symmetry breaks down to $U(1)_Y$ by the vacuum expectation value (VEV) of a scalar field Φ on the Planck brane.

At a low-energy scale, relevant parameters in the QCD sector of this model are k, the warp factor $z_L = e^{kL}$ which represents the scale of hierarchy between the Planck and the TeV brane, 5D strong gauge coupling g_C, bulk mass parameters c_q, and brane mass ratios $\tilde{\mu}^q/\mu_2^q$. The g_C is related to 4-dimensional strong gauge coupling as $g_s = g_C/\sqrt{L}$. Basically, c_q controls the localization of the zero mode wave functions near the TeV brane and the Planck brane. $\tilde{\mu}^q$ and μ_2^q are induced by VEVs of the scalar filed Φ. Brane mass matrices are regarded as flavor diagonal so that the flavor mixing is turned off in this paper. Our setup follows in Ref. [14], and unknown parameters are $(k, z_L, c_q, \tilde{\mu}^q/\mu_2^q)$ at low energy. Three of these parameters can be fixed by taking electroweak coupling α_W, W boson mass m_W, and quark mass m_q. One parameter of $(k, z_L, c_q, \tilde{\mu}^q/\mu_2^q)$ remains as a free parameter, and we take z_L as an input parameter. In this paper we consider two cases of $z_L = 10^{15}$ and $z_L = 10^{20}$. Once the z_L parameter is fixed, Higgs mass is determined. When we input z_L as $z_L = 10^{15}$ and 10^{20}, Higgs mass is calculated as $m_H = 135$ GeV and 158 GeV when $\theta_H = \frac{\pi}{2}$, respectively, where θ_H is the Wilson line phase which gives a nonvanishing VEV of Higgs. This is not compatible with recent experimental data, and the suitable Higgs mass can be obtained when $\theta_H \neq \frac{\pi}{2}$. Such θ_H might be realized by taking specific matter content,[2] and the QCD sector is not affected by such modification of the model. We focus on the QCD sector of this model, and therefore, our analysis is not conflicted with the observed m_H.

[2]When $\theta_H = \frac{\pi}{2}$, Z_2 symmetry called H-parity is dynamically emerged, and Higgs boson can be dark matter. Observed Higgs boson mass can be realized by $\theta_H \neq \frac{\pi}{2}$, where the model becomes realistic as shown in Ref. [16].

In the $SO(5) \times U(1)$ gauge-Higgs unification model, parity is violated in the QCD process because of the difference between q_L-$\bar{q}_L$-$G^{(n)}$ and q_R-$\bar{q}_R$-$G^{(n)}$ couplings. As we show in Sec. III, the latter coupling is much larger than the former one. This is because that q_R (q_L) wave function is located near the TeV (the Planck) brane, and KK gluon is located near the TeV brane. Such a configuration of a quark wave function is related to brane mass parameters induced by VEVs of Φ on the Planck brane. Only the left-handed quark has brane mass terms, and mixes with extra particles located on the Planck brane. These chiral interactions induce a sizable parity violation in the QCD process, which can be discovered at the LHC. In order to investigate this parity violation, we focus on the helicity dependence of top pair production at the LHC.

III. EXPERIMENTAL OBSERVABLES AT LHC

A. Production cross sections

First, we prepare parameter sets of the model. Parity violation in the QCD process arises from one KK gluon exchange at tree level, which the process is $q\bar{q} \to G^{(n)} \to t\bar{t}$. KK gluon masses and their total decay widths are shown in Table I with $z_L = 10^{15}$ and Table I with $z_L = 10^{20}$. The couplings of KK gluon to quarks are listed in Table II, where $g_q^{G^{(n)}}$ represents the q-$\bar{q}$-$G^{(n)}$ coupling constants in unit $g_s = g_C/\sqrt{L}$. c_q and $\tilde{\mu}^q/\mu_2^q$ are given in Table III.

The production cross sections of the first, second, and third KK gluons with the parameters of $z_L = 10^{15}$ and 10^{20} are summarized in Table IV, where the top quark mass is 172.5 GeV and CTEQ6L PDF [17] is used for proton-proton collision at $\sqrt{s} = 8$ TeV. For simplicity, the renormalization and factorization scales are fixed at $m_Z = 90.188$ GeV, which result in the electroweak and strong coupling constants of $\alpha(m_Z) = 1/132.507$ and $\alpha_s(m_Z) = 0.1298$, respectively. The top pair production cross section of the SM prediction under the same condition is 197.6(1) pb.

Figure 1 presents the top quark p_T spectrum and the $t\bar{t}$ invariant mass system $m_{t\bar{t}}$ with the first and second KK gluons at $z_L = 10^{15}$ and $z_L = 10^{20}$ together with the SM prediction, respectively.

TABLE I. KK gluon masses and their total decay widths, Γ_{total}, with $z_L = 10^{15}$ and $z_L = 10^{20}$.

Unit GeV	1st KK gluon	2nd KK gluon	3rd KK gluon
	$z_L = 10^{15}$		
Mass	1144	2630	4111
Γ_{total}	7205	1265	274.3
	$z_L = 10^{20}$		
Mass	1330	3030	6452
Γ_{total}	10987	1615	175.7

TABLE II. The coupling constants of q-$\bar{q}$-$G^{(n)}$ with $z_L = 10^{15}$ and $z_L = 10^{20}$ in unit g_s.

Unit g_s	$n = 1$	$n = 2$	$n = 3$
	$z_L = 10^{15}$		
$g^{G^{(n)}}_{u_L}$	−0.195	0.133	−0.108
$g^{G^{(n)}}_{c_L}$	−0.195	0.133	−0.108
$g^{G^{(n)}}_{t_L}$	0.442	−0.402	0.295
$g^{G^{(n)}}_{d_L}$	−0.195	0.133	−0.108
$g^{G^{(n)}}_{s_L}$	−0.195	0.133	−0.108
$g^{G^{(n)}}_{b_L}$	0.661	−0.370	0.283
$g^{G^{(n)}}_{u_R}$	6.323	2.129	0.734
$g^{G^{(n)}}_{c_R}$	6.044	1.633	0.568
$g^{G^{(n)}}_{t_R}$	5.603	0.949	0.408
$g^{G^{(n)}}_{d_R}$	6.323	2.129	0.734
$g^{G^{(n)}}_{s_R}$	6.044	1.633	0.568
$g^{G^{(n)}}_{b_R}$	5.500	0.832	0.417
	$z_L = 10^{20}$		
$g^{G^{(n)}}_{u_L}$	−0.168	0.114	0.079
$g^{G^{(n)}}_{c_L}$	−0.168	0.114	0.079
$g^{G^{(n)}}_{t_L}$	0.366	−0.367	−0.221
$g^{G^{(n)}}_{d_L}$	−0.168	0.114	0.079
$g^{G^{(n)}}_{s_L}$	−0.168	0.114	0.079
$g^{G^{(n)}}_{b_L}$	0.563	−0.334	−0.213
$g^{G^{(n)}}_{u_R}$	7.158	2.174	0.455
$g^{G^{(n)}}_{c_R}$	6.900	1.733	0.369
$g^{G^{(n)}}_{t_R}$	6.518	1.143	0.250
$g^{G^{(n)}}_{d_R}$	7.158	2.174	0.455
$g^{G^{(n)}}_{s_R}$	6.900	1.733	0.369
$g^{G^{(n)}}_{b_R}$	6.430	1.039	0.234

TABLE III. Bulk mass parameters c_q and brane mass ratios $\tilde{\mu}^q/\mu_2^q$ with $z_L = 10^{15}$ and $z_L = 10^{20}$.

	c_q			$\tilde{\mu}^q/\mu_2^q$		
z_L	(u, d)	(c, s)	(t, b)	(u, d)	(c, s)	(t, b)
10^{15}	0.843	0.679	0.432	2.283	0.0889	0.0173
10^{20}	0.757	0.634	0.451	2.283	0.0889	0.0172

TABLE IV. Production cross sections of the first, second and third KK-gluons with the parameters of $z_L = 10^{15}$ and 10^{20} in a unit of pb. The top quark mass is 172.5 GeV and CTEQ6L PDF is used for proton-proton collision at $\sqrt{s} = 8$ TeV. The Standard Model top pair production cross section is 197.6(1) pb under same condition.

Unit pb	1st KK gluon	2nd KK gluon	3rd KK gluon
$z_L = 10^{15}$	22.61(2)	0.1573(2)	$6.45(1) \times 10^{-6}$
$z_L = 10^{20}$	12.67(1)	0.1065(1)	$8.50(1) \times 10^{-8}$

Although the figures at $z_L = 10^{15}$ are similar to those at $z_L = 10^{20}$, we can notice that KK gluon contributions of the former are larger than those of the latter.

All parts of Fig. 1 show that the SM contribution is suppressed in high p_T or $m_{t\bar{t}}$ regions, and the first KK gluon production process becomes almost dominant. The top pair production cross section is precisely measured within a 10% level [18]. Given the fact that the theoretical uncertainty also gives similar uncertainty at next-to-next-to-leading order calculation [19], the shown production cross sections in the table are nearly on the border of the experimental uncertainty. The differential cross section measurements [20] as a function of top quarks p_T or $m_{t\bar{t}}$ will allow us to explore a wide range of the parameter space of this model.

B. Asymmetry measurement

Now let us estimate QCD parity violation in the gauge-Higgs unification model. The left-right asymmetry is given as

$$A_{\mathrm{LR}} = \frac{N(t_L\bar{t}_L) - N(t_R\bar{t}_R)}{N(t_L\bar{t}_L) + N(t_R\bar{t}_R)}, \tag{3.1}$$

where N is the number of events with a left- or right-handed helicity state of the t ($t_{L/R}$) and $\bar{t}$ ($\bar{t}_{L/R}$) quarks. First, we present the left-right asymmetry A_{LR} as a function of the $t\bar{t}$ invariant mass system in Fig. 2. The first, second, and third KK gluons are interfered with by the SM processes. We take the parameters $z_L = 10^{15}$ and 10^{20} as samples, and both cases are shown in the figure. There is a very strong correlation in the asymmetric behavior of the left- and right-handed helicity states of the $t\bar{t}$ production in the gauge-Higgs unification model, while there is no asymmetric behavior in the SM prediction. This is expected that the KK gluons are strongly coupled with the right-handed top quark. This asymmetric behavior in Fig. 2 can be quantitatively understood as follows. In the high-energy limit, A_{LR} becomes

$$A_{\mathrm{LR}} \sim \frac{(g^{G^{(n)}}_{t_L})^2 - (g^{G^{(n)}}_{t_R})^2}{(g^{G^{(n)}}_{t_L})^2 + (g^{G^{(n)}}_{t_R})^2}. \tag{3.2}$$

Thus, A_{LR} is close to -1 because $g^{G^{(n)}}_{t_L}$ is much smaller than $g^{G^{(n)}}_{t_R}$. Even with the higher-order correction, the SM only predicts at most less than 2% [10]. Therefore, the size of the asymmetry might be sufficient to observe in the experiment. However, the t ($\bar{t}$) quark is immediately decayed into the final state particles without suffering the strong interaction, so that the correlation of the helicity state in the $t\bar{t}$ production is only known through the observation of the asymmetry of the final state particles ($t \to bq\bar{q}/bl\nu$). We focus on charge asymmetry and forward-backward asymmetry defined in Eqs. (3.3) and (3.4) as observable

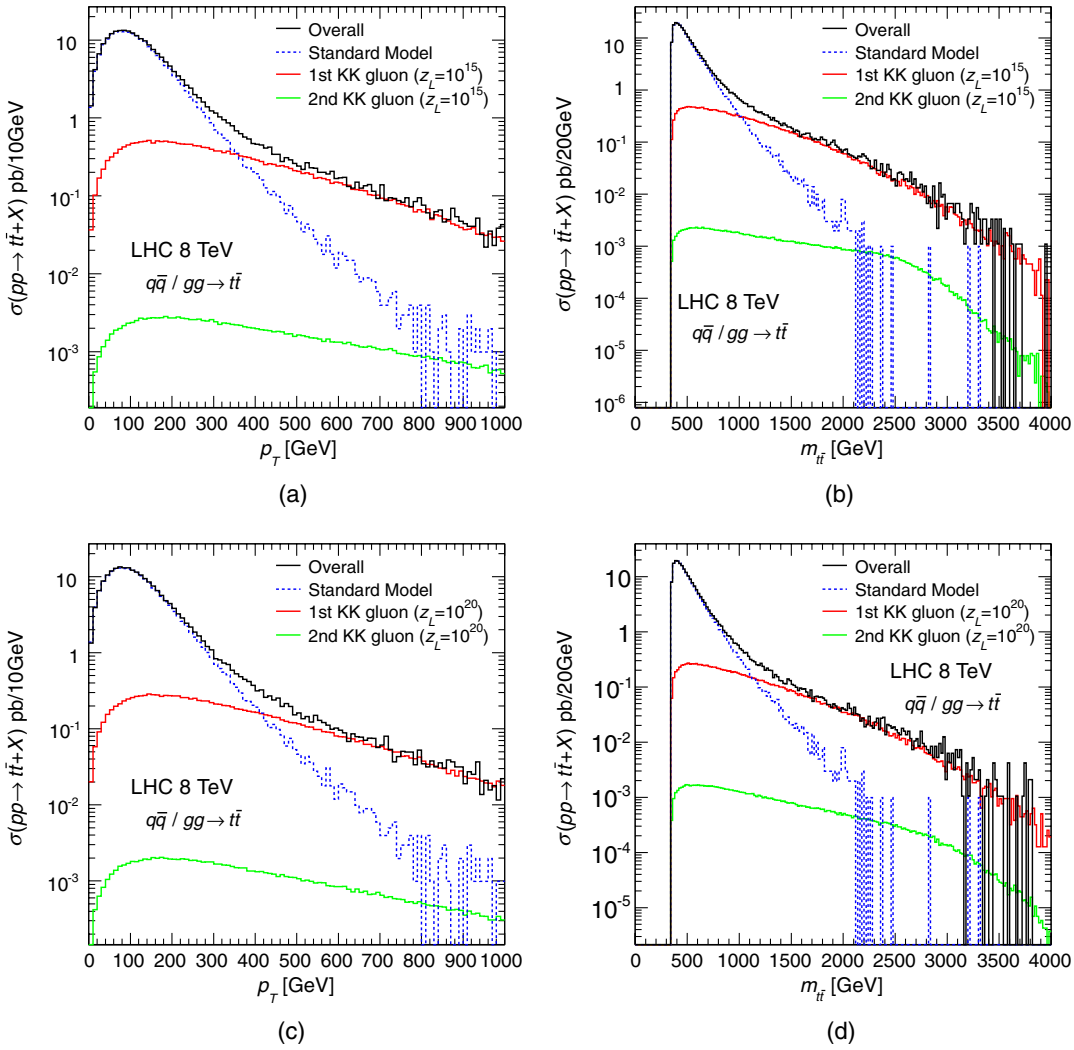

FIG. 1 (color online). (a) top quark p_T spectrum and (b) $t\bar{t}$ invariant mass system $m_{t\bar{t}}$ with the first and second KK gluons at $z_L = 10^{15}$. (c) and (d) are $z_L = 10^{20}$ case.

quantities. These two asymmetries can access a distribution of the asymmetry of t ($\bar{t}$) flight direction [21], which is caused by parity violation ($A_{\rm LR}$).

The matrix element [22] of the top pair productions is considered up to the final state particles involving a decay of the t ($\bar{t}$) quark, so that the helicity state in the t ($\bar{t}$) quark in production is properly propagated into the final state particles, and thus the event kinematics could be experimentally modeled. For simplicity, the event selections listed in Table V are applied based on the experimental signatures, where the events are categorized as "lepton + jets" and "dilepton" channels based on the W boson decay from the t and $\bar{t}$ quarks. The lepton + jets channel requires at least one high p_T electron or muon in the fiducial volume in the detector. The $|\eta| < 2.5$ is chosen by the coverage of typical tracking detectors. The b quark and the other quarks from W boson decay are considered as a jet which has to be p_T larger than 20 GeV

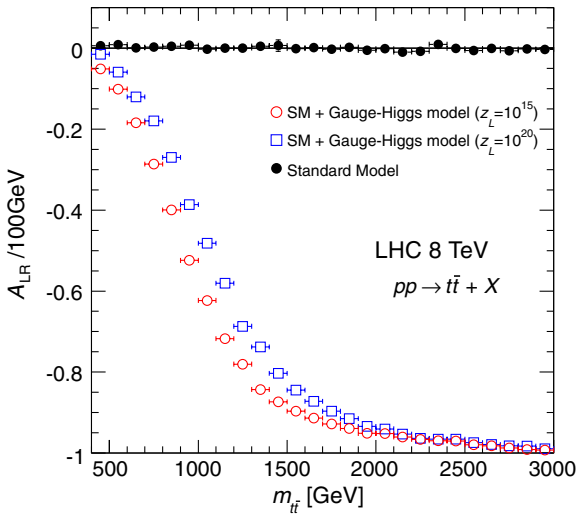

FIG. 2 (color online). Left-right asymmetry, $A_{\rm LR}$, as a function of the $t\bar{t}$ invariant mass system.

TABLE V. Event selections, which categorized as lepton + jets and dilepton channels based on the W boson decay from the t and $\bar{t}$ quarks.

Channel	Event selection
Lepton + jets channel	$p_T > 20$ GeV, $\|\eta\| < 2.5$ for lepton and quarks
Dilepton channel	$p_T > 20$ GeV, $\|\eta\| < 2.5$ for leptons and quarks
	$\sqrt{\sum_{\nu,\bar{\nu}} p_x^2 + \sum_{\nu,\bar{\nu}} p_y^2} > 50$ GeV for neutrinos

with in $|\eta| < 2.5$. The b jet tagging might enhance the top pair events against background processes. In the dilepton channel, two leptons (e or μ) are required in the final state. To further suppress the SM background processes, the missing transverse energy, which is the vectored summation of two neutrino momenta in the transverse plane, is required to be larger than 50 GeV. In the experiment, the unfolding procedure is applied to the observed experimental quantities, and here we only evaluate the 4-vector level event topology to see if given event selections are still feasible to observe the $t\bar{t}$ asymmetry to probe this model.

Based on these event selections, we define the quantities of the $t\bar{t}$ asymmetry as follows:

$$A_C = \frac{N(\Delta|y| > 0) - N(\Delta|y| < 0)}{N(\Delta|y| > 0) + N(\Delta|y| < 0)}, \qquad \Delta|y| \equiv |y_t| - |y_{\bar{t}}| \tag{3.3}$$

for the lepton + jets channel, and

$$A_{\mathrm{FB}} = \frac{|\cos\theta^+_{\mathrm{lep}}| - |\cos\theta^-_{\mathrm{lep}}|}{|\cos\theta^+_{\mathrm{lep}}| + |\cos\theta^-_{\mathrm{lep}}|} \tag{3.4}$$

for the dilepton channel, respectively. The A_C is known as the charge asymmetry and A_{FB} is the forward-backward asymmetry. The A_C is the difference of the events with the t ($\bar{t}$) quark rapidities, which is parametrized by $\Delta|y|$. The t ($\bar{t}$) quark direction is reconstructed by three jets from the t ($\bar{t}$) quark decay. In the dilepton channel, t ($\bar{t}$) quark momentum cannot be determined. Meanwhile, it is easy to see the charged lepton momentum, and charged leptons in the final state are expected to maintain the asymmetry of t and $\bar{t}$ direction. Note that A_{FB} of (3.4) is not the same observable at the Tevatron because an absolute value of t ($\bar{t}$) flight direction is meaningful at the LHC. A_{FB} is formed by the event-by-event basis with the positive and negative charged lepton direction.

Figure 3(a) shows the charge asymmetry and Fig. 3(b) shows forward-backward asymmetry as a function of the invariant mass of the $t\bar{t}$ system, and dilepton mass system after event selections applied for lepton + jets and dilepton channels, respectively. We demonstrate the asymmetries when the gauge-Higgs unification model is included in the SM processes. We also estimate that the integrated A_C is -0.04. As for A_{FB}, it reaches -0.1 in high m_{ll} region. With 5%–10% asymmetry, this is experimentally still sufficient to observe [20].

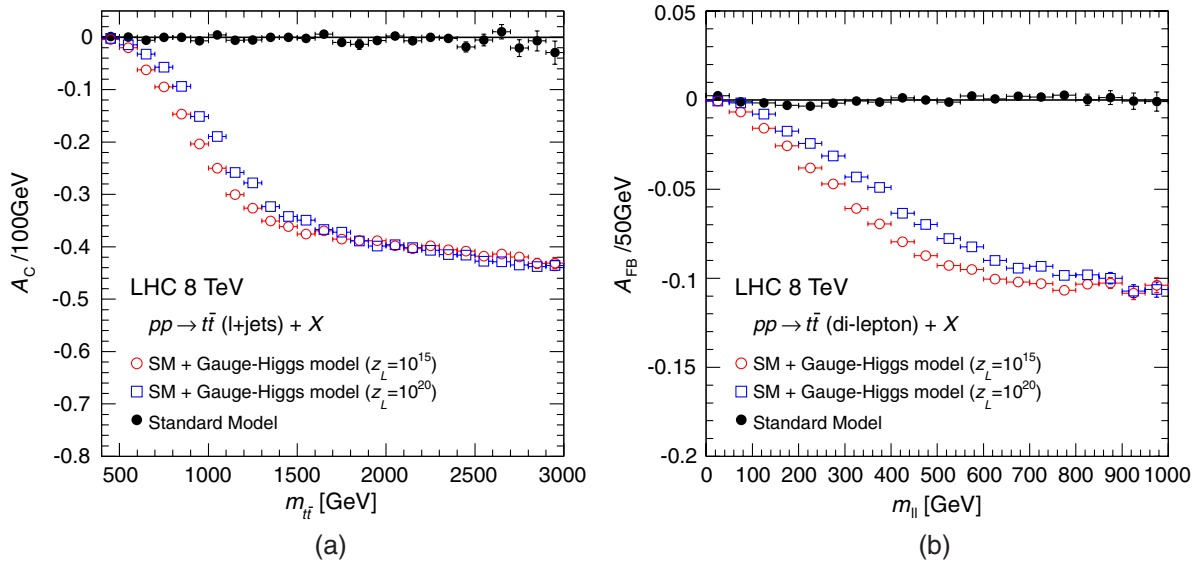

FIG. 3 (color online). (a) charge asymmetry and (b) forward-backward asymmetry as a function of the invariant mass of the $t\bar{t}$ system, after event selections applied for lepton + jets and dilepton channels, respectively.

IV. CONCLUSION

We have discussed the parity violation in QCD in the warped extra dimension model where Higgs and KK gluons are localized on the TeV brane and left- and right-handed fermions have different configurations in the bulk. In this setup, parity is violated in the QCD sector at tree level, which can be observed by the helicity asymmetry of $t\bar{t}$ at the LHC. We pick up the $SO(5) \times U(1)$ gauge-Higgs unification model as a concrete model, and find that large helicity asymmetry appears at the high $m_{t\bar{t}}$ region. We have evaluated LHC observable quantities, A_C and $A_{\rm FB}$, which can reach -0.4 and -0.1, respectively, with specific parameters in a high-energy region. We have also estimated the integrated A_C at -0.04 for all $m_{t\bar{t}}$ region. Clearly, it is larger than the SM background, and it is sufficient to be experimentally observed. Furthermore, note that the threshold behavior of the asymmetry in the $t\bar{t}$ invariant mass system is proportional to the first KK gluon mass. We comment on the case of $\theta_H \neq \frac{\pi}{2}$ for realistic Higgs mass. In this case the z_L factor might be changed, however, the asymmetric behavior is similar to our result since the relation $g_{q_R}^{G^{(n)}} \gg g_{q_L}^{G^{(n)}}$ is maintained.

In the experimental side, $A_{\rm FB}$ is not yet reported at the LHC. However, it is important because the dilepton channel is expected to be a probe of the $t\bar{t}$ asymmetry as we discussed in Sec. III B. As for A_C measurement, statistics are not sufficient in the $m_{t\bar{t}} > 450$ GeV region. Thus, in this region, only an integrated A_C is reported. The measured charge asymmetry A_C is consistent with our calculation [23], however, total error (statistic and systematic) is still large ($\sim 5\%$). Statistic and systematic errors are approximately ± 0.03(stat) and ± 0.02(syst), respectively. It is necessary to distinguish the KK gluon contribution from the SM background. The SM prediction of A_C is given by $A_C^{\rm SM} = 0.00115 \pm 0.0006$ [24]. Then we can recognize the asymmetry to be KK gluon contribution when errors are suppressed as ~ 0.01. In order to obtain ~ 0.01 statistic error, the integrated luminosity needs to be ~ 100 fb^{-1}. While, if the systematic error reduces about $1/10$, it is possible to distinguish the A_C evaluated in this paper from the SM background. Therefore, A_C is a promising observable for the KK gluon contribution. $A_{\rm FB}$ is also a hopeful observable in the dilepton channel, and the precise measurements of A_C and $A_{\rm FB}$ at the LHC are important to determine the coupling structure of this model.

ACKNOWLEDGMENTS

We thank Y. Hosotani for helpful discussions. This work is partially supported by Scientific Grant by Ministry of Education and Science, Grants No. 22011005, No. 24540272, No. 20244028, and No. 21244036. The works of K. K. are supported by Research Fellowships of the Japan Society for the Promotion of Science for Young Scientists.

[1] G. Aad *et al.* (ATLAS Collaboration), Phys. Lett. B **716**, 1 (2012); S. Chatrchyan *et al.* (CMS Collaboration), *ibid.* **716**, 30 (2012).

[2] N. Cabibbo, L. Maiani, G. Parisi, and R. Petronzio, Nucl. Phys. **B158**, 295 (1979).

[3] J. Elias-Miro, J. R. Espinosa, G. F. Giudice, G. Isidori, A. Riotto, and A. Strumia, Phys. Lett. B **709**, 222 (2012).

[4] A. Djouadi, Phys. Rep. **457**, 1 (2008).

[5] L. Randall and R. Sundrum, Phys. Rev. Lett. **83**, 3370 (1999).

[6] Y. Grossman and M. Neubert, Phys. Lett. B **474**, 361 (2000); T. Gherghetta and A. Pomarol, Nucl. Phys. **B586**, 141 (2000); S. Chang, C. S. Kim, and M. Yamaguchi, Phys. Rev. D **73**, 033002 (2006); M. E. Albrecht, M. Blanke, A. J. Buras, B. Duling, and K. Gemmler, J. High Energy Phys. 09 (2009) 064.

[7] S. J. Huber, Nucl. Phys. **B666**, 269 (2003); K. Agashe, G. Perez, and A. Soni, Phys. Rev. D **71**, 016002 (2005); M. S. Carena, A. Delgado, E. Ponton, T. M. P. Tait, and C. E. M. Wagner, Phys. Rev. D **71**, 015010 (2005); E. De Pree and M. Sher, Phys. Rev. D **73**, 095006 (2006); M. S. Carena, E. Ponton, J. Santiago, and C. E. M. Wagner, Nucl. Phys. B759, 202 (2006); G. Cacciapaglia, C. Csaki, J. Galloway, G. Marandella, J. Terning, and A. Weiler, J. High Energy Phys. 04 (2008) 006; C. Csaki, A. Falkowski, and A. Weiler, Phys. Rev. D **80**, 016001 (2009); S. Casagrande, F. Goertz, U. Haisch, M. Neubert, and T. Pfoh, J. High Energy Phys. 10 (2008) 094; M. E. Albrecht, M. Blanke, A. J. Buras, B. Duling, and K. Gemmler, J. High Energy Phys. 09 (2009) 064; M. Bauer, F. Goertz, U. Haisch, T. Pfoh, and S. Westhoff, J. High Energy Phys. 11 (2010) 039.

[8] B. Lillie, L. Randall, and L.-T. Wang, J. High Energy Phys. 09 (2007) 074; B. Lillie, J. Shu, and T. M. P. Tait, Phys. Rev. D **76**, 115016 (2007); A. Djouadi, G. Moreau, and R. K. Singh, Nucl. Phys. **B797**, 1 (2008).

[9] T. Stelzer and S. Willenbrock, Phys. Lett. B **374**, 169 (1996); M. Beneke, I. Efthymiopoulos, M. L. Mangano, J. Womersley, A. Ahmadov, G. Azuelos, U. Baur, A. Belyaev *et al.*, arXiv:hep-ph/0003033; W. Bernreuther, A. Brandenburg, Z. G. Si, and P. Uwer, Phys. Rev. Lett. **87**, 242002 (2001); Nucl. Phys. **B690**, 81 (2004); W. Bernreuther, M. Fucker, and Z.-G. Si, Phys. Rev. D **74**, 113005 (2006); W. Bernreuther, J. Phys. G **35**, 083001 (2008).

[10] W. Beenakker, A. Denner, W. Hollik, R. Mertig, T. Sack, and D. Wackeroth, Nucl. Phys. **B411**, 343 (1994); C. Kao and D. Wackeroth, Phys. Rev. D **61**, 055009 (2000); W. Bernreuther, M. Fucker, and Z. G. Si, Phys. Rev. D **78**, 017503 (2008).

[11] N. Haba, K. Kaneta, S. Matsumoto, T. Nabeshima, and S. Tsuno, Phys. Rev. D **85**, 014007 (2012).

[12] N. Haba, K. Kaneta, and T. Onogi, arXiv:1109.5442.

[13] K. Agashe, R. Contino, and A. Pomarol, Nucl. Phys. **B719**, 165 (2005); A. D. Medina, N. R. Shah, and C. E. M. Wagner, Phys. Rev. D **76**, 095010 (2007); Y. Hosotani, K. Oda, T. Ohnuma, and Y. Sakamura, Phys. Rev. D **78**, 096002 (2008); **79**, 079902(E) (2009); Y. Hosotani, S. Noda, and N. Uekusa, Prog. Theor. Phys. **123**, 757 (2010).

[14] Y. Hosotani, M. Tanaka, and N. Uekusa, Phys. Rev. D **84**, 075014 (2011).

[15] M. Blanke, A. J. Buras, B. Duling, S. Gori, and A. Weiler, J. High Energy Phys. 03 (2009) 001; A. J. Buras, Proc. Sci., KAON 09 (2009) 045.

[16] S. Funatsu, H. Hatanaka, Y. Hosotani, Y. Orikasa, and T. Shimotani, arXiv:1301.1744.

[17] J. Pumplin, D. R. Stump, J. Huston, H. L. Lai, P. M. Nadolsky, and W. K. Tung, J. High Energy Phys. 07 (2002) 012.

[18] V. Khachatryan *et al.* (CMS Collaboration), Phys. Lett. B **695**, 424 (2011); G. Aad *et al.* (ATLAS Collaboration), Phys. Lett. B **717**, 89 (2012).

[19] N. Kidonakis, arXiv:1205.3453.

[20] P. Silva *et al.* (ATLAS Collaboration and CMS Collaboration), arXiv:1206.2967.

[21] E. L. Berger, Q.-H. Cao, C.-R. Chen, and H. Zhang, arXiv:1209.4899.

[22] S. Tsuno, T. Kaneko, Y. Kurihara, S. Odaka, and K. Kato, Comput. Phys. Commun. **175**, 665 (2006).

[23] S. Chatrchyan *et al.* (CMS Collaboration), Phys. Lett. B **717**, 129 (2012); G. Aad *et al.* (ATLAS Collaboration), Eur. Phys. J. C **72**, 2039 (2012).

[24] J. H. Kuhn and G. Rodrigo, J. High Energy Phys. 01 (2012) 063.